Histochem Cell Biol (2005)
DOI 10.1007/s00418-005-0091-z

ORIGINAL PAPER

**Annette B. Galler · Maísa I. García Arguinzonis
Werner Baumgartner · Monika Kuhn
Albert Smolenski · Andreas Simm · Matthias Reinhard**

VASP-dependent regulation of actin cytoskeleton rigidity, cell adhesion, and detachment

Accepted: 23 September 2005

Abstract Enabled/vasodilator-stimulated phosphoprotein (Ena/VASP) proteins are established regulators of actin-based motility, platelet aggregation, and growth cone guidance. However, the molecular mechanisms involved essentially remain elusive. Here we report on a novel mechanism of VASP action, namely the regulation of tensile strength, contractility, and rigidity of the actin cytoskeleton. Compared to wild-type cells fibroblasts derived from VASP-deficient mice have thicker and more stable actin stress fibres. Furthermore focal adhesions are enlarged, myosin light chain phosphorylation is increased, and the rigidity of the filament-supported plasma membrane is elevated about three- to fourfold, as is evident from atomic force microscopy. Moreover, fibronectin-coated beads adhere stronger to the surface of VASP-deficient cells. The resistance of these beads to mechanical displacement by laser tweezers is dramatically increased in an F-actin-dependent mode. Cytoskeletal stabilization coincides with slower cell adhesion and detachment, while overall adhesion is increased. Interestingly, many of these effects observed in VASP (−/−) cells are recapitulated in VASP-overexpressing cells, hinting towards a balanced stoichiometry necessary for appropriate VASP function. Taken together, our results suggest that VASP regulates surface protrusion formation and cell adhesion through modulation of the mechanical properties of the actin cytoskeleton.

Keywords Actin cytoskeletal dynamics · Cell surface extensions · Cell surface rigidity · Mechanotransduction · Scaffold proteins

Introduction

Many cellular processes, such as migration, spreading, adhesion, and growth cone guidance, depend on regulated interactions of integrins with the extracellular matrix (ECM). In addition to ligand-induced signalling (Geiger et al. 2001; Juliano 2002) adhesion enables the cell to apply traction forces on the ECM.

Annette B. Galler, Maísa I. García Arguinzonis these authors contributed equally to this work

A. B. Galler · M. I. García Arguinzonis · M. Kuhn
A. Smolenski · A. Simm · M. Reinhard (✉)
Institute for Clinical Biochemistry and Pathobiochemistry,
University of Würzburg, Josef-Schneider-Str. 2, 97080 Würzburg, Germany
E-mail: M.Reinhard@immunoGlobe.com
Tel.: +49-9364-810610
Fax: +49-9364-810613

W. Baumgartner
Institute of Anatomy and Cell Biology, University of Würzburg,
Koellikerstr. 6, 97070 Würzburg, Germany

Present address: M. Reinhard
immunoGlobe Antikoerpertechnik GmbH,
Rudolf-Diesel-Str. 8A, 97267 Himmelstadt, Germany

Present address: A. B. Galler
Onkologie, Merck Pharma GmbH, Location: AL17/145,
Alsfelder Str. 17, 64289 Darmstadt, Germany

Present address: M. I. García Arguinzonis
Centro de Investigaciones Cardiovasculares CSIC-ICCC,
Hospital de la Santa Creu i Sant Pau - Barcelona,
Av. Antoni Maria Claret 167, 08025 Barcelona, Spain

Present address: W. Baumgartner
Department of Cellular Neurobionics, Institute of Biology 2,
RWTH-Aachen, Kopernikusstr. 16, 52056 Aachen, Germany

Present address: M. Kuhn
Rudolf-Virchow-Center and Department of Dermatology,
Molecular Cell Dynamics Group,
University of Würzburg,
Josef-Schneider-Str. 2, 97080 Würzburg, Germany

Present address: A. Smolenski
Institute for Biochemistry II, University Clinic,
Bldg. 75, Theodor-Stern-Kai 7,
60590 Frankfurt, Germany

Present address: A. Simm
Clinic for Heart and Thorax Surgery, University of Halle,
Ernst-Grube-Str. 40, 06120 Halle, Germany

Mechanical forces in conjunction with the physical resistance or compliance of the extracellular substratum are thought to act as mechanical cues. Similar to chemical environmental cues, they regulate cell behaviour and fate (Geiger and Bershadsky 2002; Geiger et al. 2001). Forces acting on integrin-mediated adhesions cause local and reversible strengthening of integrin–cytoskeleton linkages. This reinforcement is proportional to the restraining force, depends on both occupancy and clustering of integrins (Choquet et al. 1997; Geiger and Bershadsky 2002), and is correlated with a decrease in adhesion site dynamics regulated by the protein tyrosine phosphatase SHP2 (von Wichert et al. 2003).

The actin cytoskeleton not only supports cell-matrix adhesion but, in addition, the submembraneous peripheral actin filament meshwork also directly affects plasma membrane rigidity, possibly through multiple lipid–protein interactions. The connection between the cytoskeleton and the plasma membrane is subject to regulation by signalling molecules such as phosphatidylinositol-4,5-bisphosphate (PIP_2) (Raucher et al. 2000). Interestingly, PIP_2 synthesis can be regulated by the focal adhesion proteins talin and focal adhesion kinase. This has been proposed to play a potential role in membrane remodelling during cell migration and spreading (Liddington et al. 2003).

Signalling pathways impinging on integrin–cytoskeletal linkages and actin associated adaptor molecules play a critical role in modulating integrin function (reviewed in Calderwood et al. 2000). But the molecular mechanisms that lead to an orchestrated interplay between cell adhesion, mechanical properties of the cell surface, and actin filament assembly, dynamics, and contractility are poorly understood. Integrin binding to ECM proteins, like fibronectin (FN), coincides with the activation of the Rho family small GTPases Cdc42 and Rac (Price et al. 1998), which promote the formation of filopodia and lamellipodia, respectively (Nobes and Hall 1995). In contrast, Rho is transiently inhibited by adhesion to FN, but is activated during later phases of adhesion (for a review see Arthur et al. 2002). Membrane translocation of Rac in response to cell adhesion is critical for downstream Rac signalling (Abassi and Vuori 2002; del Pozo et al. 2004, 2002, 2000), such as activation of the Ser/Thr kinase PAK, which affects actin filament stabilization/destabilization via the LIM kinase–Cofilin pathway (Bamburg 1999). Other Rac targets include PIP5 K and IRSp53 that enable actin filament uncapping and WAVE-dependent activation of Arp2/3 complex with subsequent filament branching, respectively (Bishop and Hall 2000; Geiger and Bershadsky 2001; Ridley 2001).

Proteins of the enabled (Ena)/vasodilator-stimulated phosphoprotein (VASP) family appear to promote actin filament formation. Suggested mechanisms involve recruitment of polymerization competent profilin–actin complexes (Auerbuch et al. 2003; Reinhard et al. 2001), antagonism to capping protein activity (Bear et al. 2002; Krause et al. 2002), and a facilitated release of actin filament branches from a structure-bound branching enzyme (Samarin et al. 2003). As a possible consequence of the latter mechanism(s), Ena/VASP proteins decrease the relative degree of filament branching (Bear et al. 2002; Krause et al. 2002). This has been interpreted to account for the lower lamellipodial protrusion velocity and increased protrusion persistence observed in Mammalian Ena (Mena)/VASP double null cells (Bear et al. 2000, 2002). Besides this, there are a variety of other connections to cytoskeleton-related proteins that may contribute to the cytoskeletal effects of Ena/VASP proteins. Thus, Ena/VASP proteins interact with profilin, zyxin, vinculin (for a review see Reinhard et al. 2001), the Arp2/3 complex activating protein WASP (Castellano et al. 2001), and IRSp53 (Krugmann et al. 2001). Moreover, VASP is involved in the regulation of the Rac/PAK pathway (García Arguinzonis et al. 2002) and cooperates with Diaphanous (mDia) in Rho-dependent F-actin assembly (Grosse et al. 2003). Recently, proteins of the Mig10/RIAM/Lamellipodin family have been identified as candidate linkages between Ena/VASP proteins and Ras-related GTPases (Legg and Machesky 2004).

On the cellular and genetic level, *Drosophila* Ena and the *Caenorhabditis* homologue UNC-34 function in repulsive axon guidance downstream of the slit receptor roundabout (Robo)/SAX-3 and Netrin receptor UNC-5, respectively (Bashaw et al. 2000; Colavita and Culotti 1998; Yu et al. 2002). Interestingly, the Ena/VASP family member UNC-34 is also involved in UNC40/DCC Netrin receptor-dependent axon outgrowth and attraction (Gitai et al. 2003). In the mammalian system VASP-deficient platelets show increased integrin-dependent fibrinogen binding after thrombin or collagen activation and VASP is involved in the cyclic nucleotide-dependent inactivation of the integrin $\alpha_{IIb}\beta_3$ (Aszodi et al. 1999; Hauser et al. 1999). As outlined above, our current understanding of Ena/VASP protein functions does not suggest any obvious molecular mechanism(s) for this negative regulation of plasma membrane receptors, like integrins. Therefore, we initiated this study to investigate in more detail the integrin and cytoskeleton-related changes in VASP-deficient cells.

Unexpectedly, we found that both the ablation of the murine VASP gene and the overexpression of VASP led to similar effects on stress fibre morphology and stability. This indicates that VASP modulates actin filament architecture, at least in part, by mechanisms beyond a direct VASP interaction with actin filaments. Moreover, the tensile strength of the cell cortex and actin cytoskeleton was dramatically elevated and integrin-dependent adhesion was increased but delayed in VASP-deficient cells. Taken together, our results reveal that VASP affects cytoskeletal turnover or contractility, probably also on a level beyond a direct interaction with actin filaments. Our data also shed new light on

the role of Ena/VASP proteins in the modulation of membrane process formation and retraction in response to extracellular cues.

Materials and methods

Vectors and constructs

The pcDNA3 (Invitrogen) based eukaryotic expression vectors for overexpression of human VASP, N-terminally tagged with an epitope of VSV glycoprotein G, have been described elsewhere (Smolenski et al. 2000).

Cells

Mouse cardiac fibroblasts (MCFB) and mesangial cells derived from VASP(+/+) and VASP(−/−) mice, as well as reconstituted VASP(−/−) fibroblasts stably expressing human VASP have been described previously (Gambaryan et al. 2001; García Arguinzonis et al. 2002). All cell lines were grown in a humidified atmosphere containing 5% CO_2. PtK_2 cells and MCFB were cultured in DMEM (Gibco) supplemented with 10% FCS (Gibco), 100 μg/ml penicillin, and 100 μg/ml streptomycin. Mesangial cells were cultured in RPMI 1640 with 15% FCS, 100 U/ml penicillin, 100 μg/ml streptomycin, and 1% ITS liquid media supplement (Sigma). Cells were passaged by trypsinization (MCFB) or by treatment with trypsin/EDTA (Sigma) after a pre-incubation for 5–10 min in 10 mM EDTA/PBS (PtK_2 and mesangial cells). For immunofluorescence analysis of VASP-overexpressing cells, PtK_2 cells were seeded on glass coverslips and transfected at 50–80% confluence using FuGene 6 reagent (Roche). For laser tweezer experiments MCFB cells were seeded on glass coverslips and grown to confluence (2–4 days).

Cell adhesion assay

For coating with fibronectin, 96-well plates (Costar) were incubated overnight at 4°C with 0, 1, 3, 5, 10 μg/ml fibronectin (F-0895, Sigma) in PBS. The wells were blocked with 1% BSA in PBS for 2 h at room temperature, and washed twice with PBS. In the preparation of the assay, cells were harvested with 5 mM EDTA in PBS, counted, washed twice with serum-free DMEM containing 0.1% BSA, and resuspended at 10^5 cells/ml. Hundred microlitre of the cell suspension was added to each well and cells were allowed to attach for 30 min. Non-adherent cells were removed by washing twice with serum-free DMEM/1% BSA, and attached cells were permeabilized and incubated for 1 h at 37°C with 3 mg/ml Sigma 104 phosphatase substrate, 0.5% Triton X-100, 50 mM sodium acetate (pH 5.0). The reaction was completed by adding 1 volume of 1 N NaOH and the absorbance was measured at OD^{405} with a microtiter plate reader. A standard curve with known cell numbers was set up for each cell line.

Immunofluorescence

Cells were seeded at low density on coverslips, kept in medium with calf serum/FCS as indicated, washed with PBS supplemented with 0.9 mM $CaCl_2$, 0.5 mM $MgCl_2$, and were fixed with 3.7% formaldehyde (prepared from paraformaldehyde) in PBS for 20 min on ice. Cells were permeabilized for 5 min with 0.2% Triton X-100 in PBS at room temperature. After washing twice with PBS, cells were incubated for 1 h at 37°C in a moist chamber with antibodies against LPP (immunoGlobe, IG817), anti-α-Actinin 4 (immunoGlobe, IG701), mouse anti-VASP (immunoGlobe, IE273) or rabbit anti-VASP serum (immunoGlobe, M4). The cover slips were washed twice with PBS and incubated with Cy2 or Cy3 conjugated anti-rabbit IgG and Oregon green phalloidine or rhodamine phalloidine (Molecular Probes) for 1 h at 37°C in a moist chamber. After washing in PBS cover slips were rinsed in water and mounted in Mowiol 4/88 (Hoechst) solution. Samples were analysed with a digital camera using MetaMorph 4.1 software (Imaging System) connected to an Axiovert 25 or Axiovert 200 microscope.

Flow cytometry analysis of β_1 and β_3 integrins

Cells were harvested with 5 mM EDTA in PBS, counted and resuspended in PBS at 10^6 cells/ml. 10^5 cells were incubated with 50 μg/ml of FITC-conjugated hamster anti-rat CD29 or FITC-conjugated hamster anti-mouse CD61 monoclonal antibodies (PharMingen) for 10 min in the dark. The staining for β3 and β1 integrins was measured and analysed by flow cytometry using a Becton Dickinson FACSCalibur.

Two-dimensional gel electrophoresis

Mouse cardiac fibroblasts at 80% confluence were washed with PBS and harvested in Laemmli SDS-sample buffer and proteins were precipitated with chloroform/methanol as described (Wessel and Flugge 1984). Isoelectric focusing for two-dimensional gel electrophoresis was performed using the Protean® IEF cell from Biorad according to the instructions of the manufacturer. Hundred microgram of protein were solubilized in 350 μl of lysis buffer containing 7 M urea, 2 M thio-urea, 4% (w/v) CHAPS, 15 mM dithiothreitol, 0.5% carrier ampholytes pH 3–10, and 10 nM Okadaic acid. Cell extracts were loaded on a

17 cm immobilized IPG strip (Biorad), pH 3–10 (linear) using 12–24 h active re-hydration at 50 V. Focusing was carried out for 30 min at 250 V, 30 min at 500 V, 5 h at 500–4,000 V (linear) and 16 h at 4,000 V. After equilibration in 50 mM Tris, pH 8.9, 6 M urea, 30% glycerol, 2% SDS, the strips were immediately applied to vertical 12.5% SDS gels. Separated proteins were transferred onto nitrocellulose membranes (Schleicher & Schuell) and labelled with anti-MLC antibody (Santa Cruz, sc 9449) with subsequent enhanced chemoluminescence detection (Amersham-Pharmacia).

Bead preparation

Tosyl-activated superparamagnetic polystyrene beads (2.8 μm in diameter, Dynal) were coated following the instructions of the manufacturer. In brief, human fibronectin (Sigma, F 0895) was dialysed overnight against 0.1 M Na-phosphate buffer, pH 7.4 (NaPi buffer). BSA (Sigma) was solubilized at a concentration of 10 mg/ml in NaPi buffer. Fifty microliter of the bead suspension (10^8 beads) was rinsed once by pelleting and resuspension in 100 μl of NaPi buffer. Thirty microgram fibronectin or BSA was diluted to 100 μl with NaPi buffer, added to the beads and incubated for 24 h at room temperature with slow tilting rotation. The beads were washed twice for 5 min at 4°C in PBS supplemented with 0.1% (w/v) BSA, once for 24 h at room temperature in 0.1 M Na-borate buffer, pH 9.5, once for 5 min at 4°C in PBS/BSA and finally resuspended in 100 μl PBS/BSA. The beads were stored at 4°C with slow tilting rotation for 2–3 weeks and used in 1:100 dilution in serum-free medium.

Laser tweezer experiments

The home-built laser tweezers set up was used as described recently (Baumgartner et al. 2003). Briefly the TM00-beam of a Nd:YAG laser (1,064 nm) was expanded to fill the back aperture of a high NA-objective (100×1.3 oil, Zeiss), coupled through the epi-illumination port of an Axiovert 135 microscope (Zeiss) and reflected to the objective by a dicroic mirror (FT510, Zeiss). The laser intensity was adjusted to either 40 or 160 mW. Cells were transferred to FCS-free medium and protein-coated polystyrene microbeads were allowed to interact with the cell surface of monolayers for at least 5 min. Then 100–300 beads were probed during the following 5–15 min by the laser tweezers. Lateral and vertical movements were carried out using piezo-electric actuators (lateral: PXY-100; vertical: MIPOS3, Piezosystems Jena) driven by a specific high-voltage amplifier (NV 40/3S, Piezosystems Jena). Where indicated, cells were pre-incubated with 10 μM cytochalasin D (Sigma).

Atomic force microscopy

Contact mode images of living cells in DMEM medium were obtained using a Bioscope AFM driven by a Nanoscope III controller (Digital Instruments). The spring constant of the used Si_3N_4 cantilever (Park Scientific) was 0.03 N/m and scanning force was set to 3–7 nN. Force measurements were carried out in DMEM by force-distance cycles at amplitudes of 2 μm, and at a frequency of 2 Hz. For finding the appropriate position for force measurement (nucleus or lamellipodium) scanning was performed initially with 100 μm scan size. Then successive magnification steps were carried out using the built-in zoom function until approximately 100 nm scan size was reached. At the centre of this small scan area the force distance cycles were performed. Measurements were carried out at 25°C for up to 1 h.

Electron microscopy

For scanning electron microscopy cells with adhering fibronectin-coated beads were fixed for 24 h with 4% glutaraldehyde in HBSS. For easier detection of tether-like structures, in some experiments beads were aligned by a magnet placed next to the culture dish prior to and during fixation. After dehydration with a graded aceton series, critical point drying and sputter coating with palladium–gold (CPD 030, Bal-Tec) cells were examined with a DSM-962 scanning electron microscope (Zeiss).

Results

Stress fibres of both VASP-deficient and VASP-overexpressing cells are thicker and more stable

Enabled/vasodilator-stimulated phosphoprotein proteins are intimately linked to actin cytoskeleton dynamics and architecture. Therefore, we sought to investigate which aspects of the actin cytoskeleton are affected by the absence of VASP in VASP(−/−) cells. Staining MCFB with an antibody directed against the focal adhesion marker protein lipoma-preferred partner (LPP) revealed that VASP(−/−) MCFB, as compared to wild-type cells, have more prominent focal adhesion sites, both in the cell periphery and at more central positions within the cell (Fig. 1a/a′). Even more impressive results have been obtained with another microfilament protein, α-actinin. α-Actinin 1 is a prominent constituent of stress fibres, whereas it is inconsistently found associated with focal adhesions. In contrast, the second non-muscle isoform, α-actinin 4, is more readily detected at focal adhesion sites, although it does not appear to be a predominant constituent. This is evident from immunofluorescence analysis of wild-type

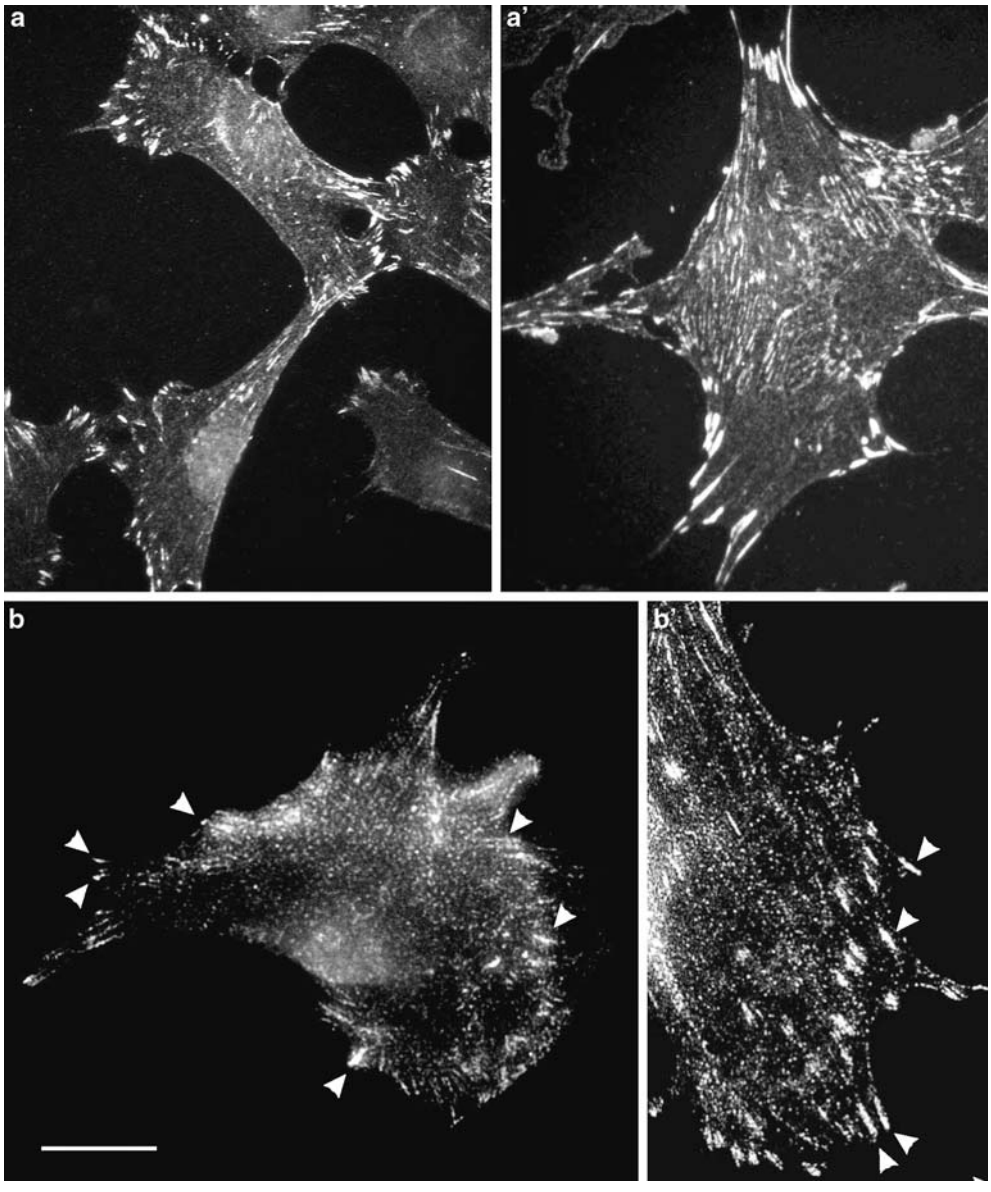

Fig. 1 Increased focal adhesion sites of VASP(−/−) cells. Focal contacts of wild-type (**a, b**) and VASP(−/−) (**a′**, **b′**) MCFB were stained for LPP (**a, a′**) and α-actinin 4 (**b, b′**), respectively. Note the more elaborated focal adhesion sites of VASP-deficient cells. *Bar* in panel B 30 μm, valid for all panels

cells using an antibody specific for the α-actinin 4 isoform (Fig. 1b). In VASP-deficient cells, however, focal adhesions are much more pronounced and are strongly decorated with α-actinin 4 (Fig. 1b′).

Also, when compared to wild-type cells, stress fibres are much thicker in a VASP(−/−) MCFB cell line (Fig. 2b), MCFB VASP(−/−) primary cells (not shown), as well as in VASP(−/−) mesangial cells (e.g. Fig. 4) than in wild-type cells (Fig. 2a). This phenotype was reverted in reconstituted VASP(−/−) MCFB (Fig. 2c), proving the absence of VASP as causal for this effect. These results were unexpected, since actin filament bundles also result from the overexpression of VASP (Fig. 2e–f and Refs. Grosse et al. 2003; Hüttelmaier et al. 1999; Price and Brindle 2000), a protein that bundles actin filaments in vitro (Bachmann et al. 1999). When VASP(−/−) cells are viewed at a larger magnification, it is obvious that filaments often appear to crossover between adjacent filament bundles (Fig. 2b insert). In VASP-overexpressing PtK2 cells (Fig. 2e/f), occasionally a very similar type of stress fibre array was found (Fig. 2e, insert). Possibly, these anastomosing stress fibres are not a particular quality of VASP-overexpressing and knockout cells, but may be just more evident in these cells due to the markedly thickened stress fibre calibre. In conclusion, as both overexpression and ablation of VASP lead to a similar morphology of thickened stress fibres, it is obvious that mechanisms other than the actin filament-bundling activity of VASP must be involved. Therefore, VASP may regulate signalling pathways, which in turn affect the shaping and architecture of stress fibres. To investigate this possibility in more detail, we analysed the phosphorylation state of myosin light chains in these cells.

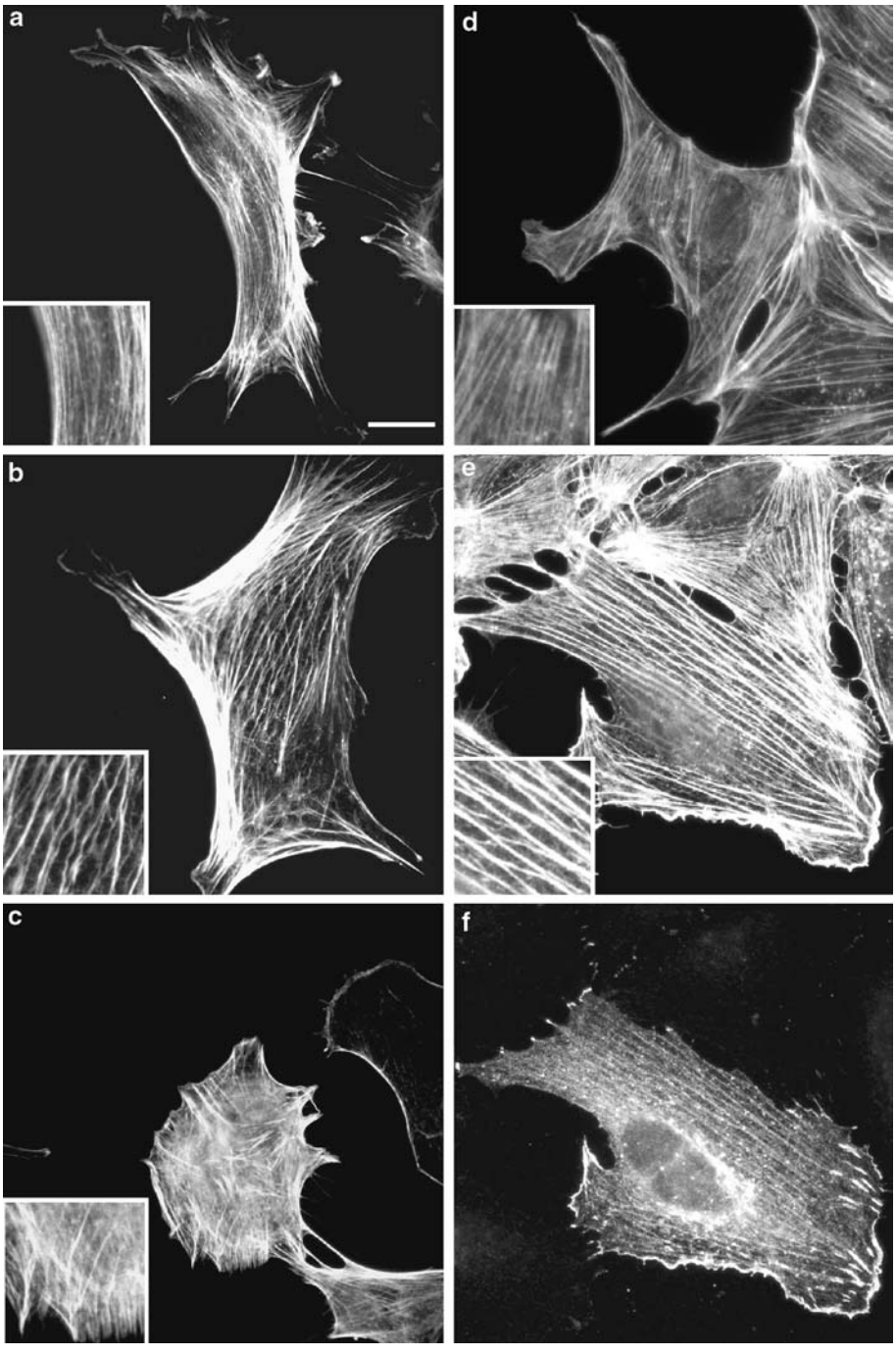

Fig. 2 Stress fibre morphology in VASP(−/−) and VASP-overexpressing cells. VASP(+/+) (**a**), VASP(−/−) (**b**), and VASP(−/−) MCFB stably transfected with a plasmid encoding human VASP (**c**), as well as control (**d**) and VASP-overexpressing (**e, f**) PtK_2 cells were stained for F-actin with Oregon Green phalloidine (**a**–**e**) and for VASP (**f**). *Insets* in panels **a**–**d** show a detailed view of the stress fibres. Note the thin actin filaments that are exchanging between different filament bundles, in particular in VASP(−/−) cells. *Bar* 15 μm

Basal myosin light chain phosphorylation is increased in VASP-deficient cells

In non-muscle cells the balance between myosin light chain (MLC) phosphorylation and dephosphorylation is a key element in the regulation of actin–myosin filament assembly and contractility (Fukata et al. 2001). MLC is phosphorylated and activated by myosin light chain kinase (MLCK) on Ser-19 and Thr-18 and by PAK-2 on Ser-19 (Chew et al. 1998). Besides increasing MLC phosphorylation through direct and indirect inhibition of myosin phosphatase, Rho-kinase also directly phosphorylates MLC at Ser-19 (Fukata et al. 2001). Since major actin filament-regulating pathways converge on MLC phosphorylation/dephosphorylation, we analysed the MLC phosphorylation state in VASP-deficient cells. MLC of VASP-deficient and wild-type cell lysates was separated and analysed by two-dimensional gel electrophoresis. For the analysis of MLC phosphorylation under unstimulated conditions, MCFB cells were starved for 24 h in 0.2% serum. MLC appeared as a series of isoelectric variants (Fig. 3b). In VASP(−/−) cells the relative intensity of the most acidic spot (marked with an arrow in Fig. 3b) was markedly in-

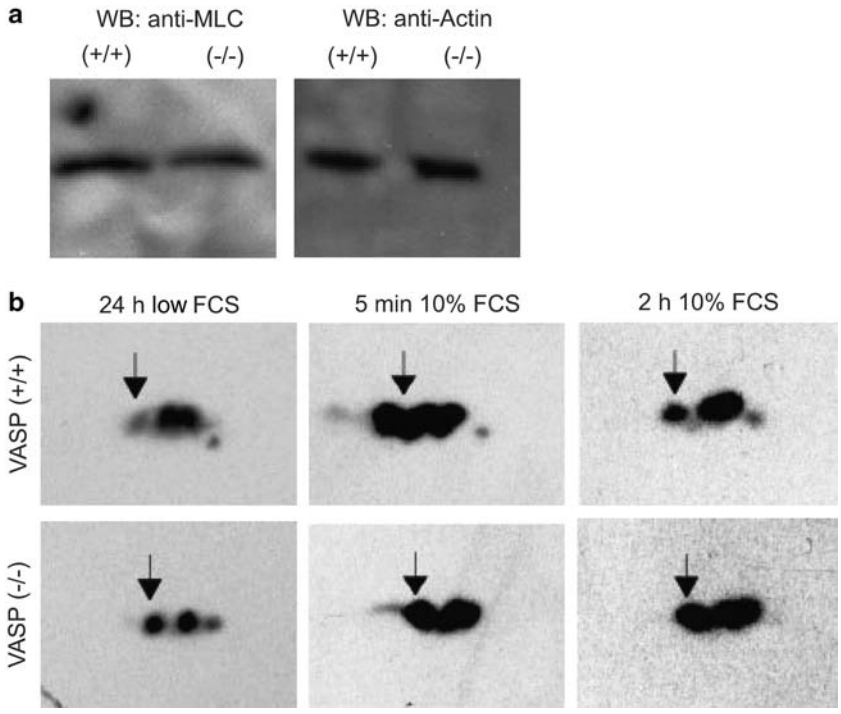

Fig. 3 Myosin light chain expression and phosphorylation in VASP(−/−) cells during serum starvation. **a** The expression level of myosin light chain is not significantly different in VASP(−/−) and wild-type MCFB when compared to an actin control. **b** VASP-deficient and wild-type cells MCFB were serum starved for 24 h (DMEM with 0.2% FCS) followed by stimulation with 10% FCS for the times indicated. Myosin light chain phosphorylation was analysed by two-dimensional gel analysis and immunoblotting

creased, indicating elevated MLC phosphorylation in these cells. This spot could also be labelled with an antibody specific for the Thr-18/Ser-19 diphosphorylated species (not shown). After serum stimulation MLC phosphorylation transiently increased in wild-type cells, whereas no major change in the relative intensities of the spots was observed in VASP(−/−) cells (Fig. 3 b).

In contrast to MLC phosphorylation, the protein expression level of MLC in MCFB was not changed when compared to an actin standard used as an internal control (Fig. 3a).

Stress fibres persist after serum starvation of both VASP-deficient and VASP-overexpressing cells

Serum deprivation is known to lead to stress fibre break down and disassembly. Indeed, after 24 h of serum starvation VASP(+/+) cells lost most of their prominent stress fibres and showed only thin actin filament structures (Fig. 4, upper panel). Within 5 min after addition of serum, stress fibres reappeared in these cells. In contrast, VASP(−/−) cells mostly maintained their stress fibre structures during starvation with a similar morphology as in the presence of serum (Fig. 4, upper panel). Similar results have been obtained with VASP-deficient mesangial cells (Fig. 4, lower panel). These morphological observations are in agreement with the biochemical data on MLC phosphorylation. Thus, in the absence of VASP stress fibres are present even after a long period of serum starvation, suggesting that VASP is required for effective stress fibre turnover. Similarly, overexpression of VASP in transiently transfected PtK_2 cells resulted in an analogous persistence of stress fibres even after serum deprivation (Fig. 5). Interestingly, a VASP mutant, in which all three phosphorylation sites (Ser-157, Ser-239, Thr-278) for cyclic nucleotide-dependent protein kinases were mutated to alanines (AAA-VASP), was also effectively inducing thick actin filament bundles (not shown). After 2–3 days, in a fraction of the cells overexpressing VASP, in particular AAA-VASP, several F-actin-containing fibres appeared as if they were wrapped around the nucleus (Fig. 5, upper panels). A closer inspection reveals that some of these actin bundles show a screw thread-like appearance (Fig. 5, inset in the upper right frame). We assume that these structures may represent collapsed but stable microfilament cables that shrivel upon detachment or rupture and get entangled around the nucleus. Regularly, similar atypical perinuclear microfilaments were observed in a wide variety of cell types, such as SF 21 cells highly overexpressing wild-type epitope tagged VASP (T. Mund, T. Jarchau, unpublished observations), as well as in VASP-overexpressing NIH 3T3 and human umbilical vein endothelial cells (not shown). Taken together, our data indicate that a balanced level of VASP expression is essential to enable stress fibre dynamics, and VASP phosphorylation may partially alleviate the stabilizing effect of the overexpressed protein.

Adhesion and detachment rates decrease in VASP(−/−) cells

The observations described above raised the question whether stress fibre stabilization is a manifestation of a more general impairment of actin cytoskeleton remodelling. To investigate this in more detail, we performed adhesion assays with fibronectin as an extracellular matrix. When low concentrations of fibronectin (1 μg/

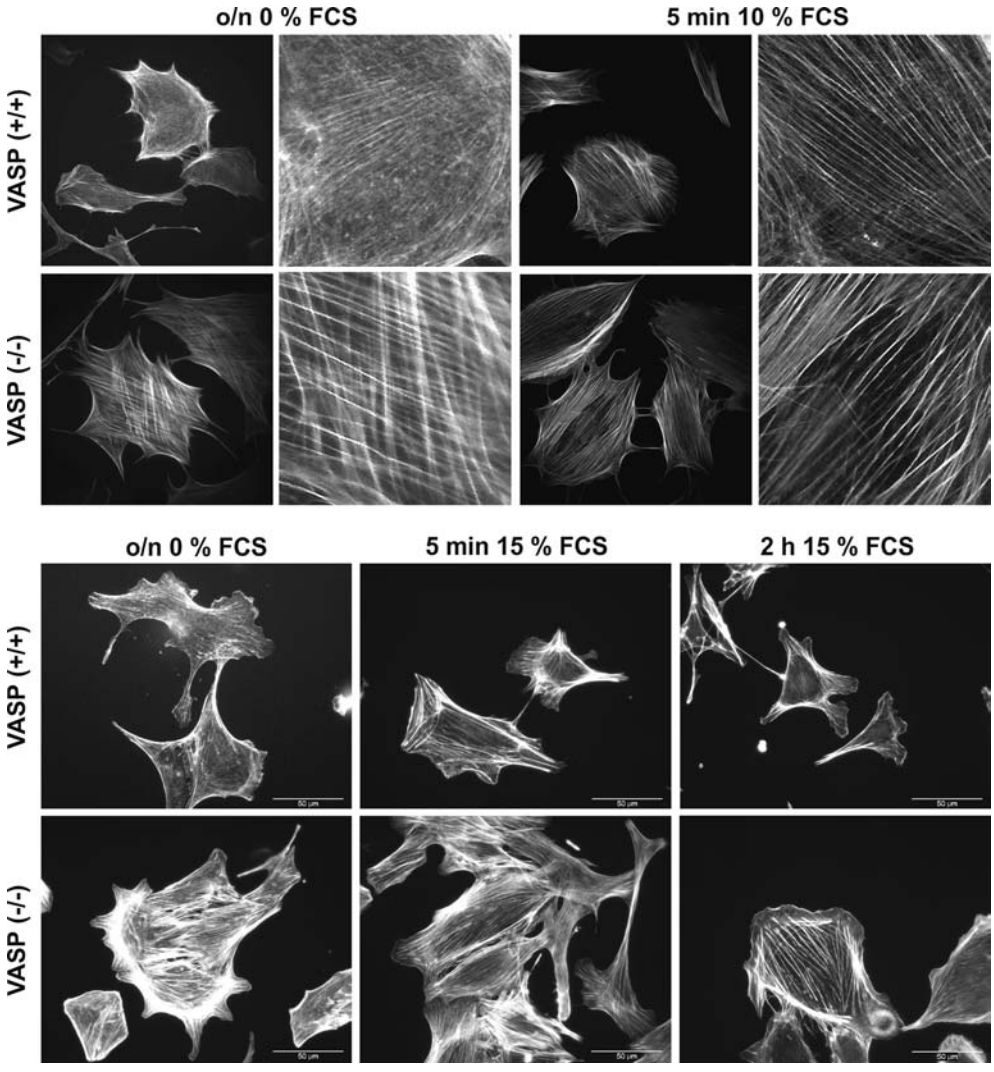

Fig. 4 Stress fibre persistence in VASP(−/−) cells during serum starvation. *Upper panel* VASP(+/+) and VASP(−/−) MCFB were starved for 24 h followed by 5 min of serum stimulation (10% FCS). Stress fibres were visualized by rhodamine phalloidine staining of F-actin. Note the thicker stress fibres of knockout cells as compared to wild-type cells. The *right part* of each pair of micrographs represents an enlargement of a selected area of the left image. *Lower panel* VASP(+/+) and VASP(−/−) mesangial cells were starved for 24 h followed by 5 min or 2 h of serum stimulation (15% FCS). Stress fibres were visualized by Oregon Green phalloidine staining of F-actin

ml) were used to coat the culture dishes, the number of VASP(−/−) MCFB adhering to the substratum within the first 30 min after seeding was about 60% of that of the corresponding wild-type cells. (Fig. 6a), while at higher concentrations of fibronectin this difference in adhesion rate was equalized (Fig. 6b). Finally, after 2–3 h both cell types attached almost quantitatively, also at 1 μg/ml fibronectin (data not shown). This indicates that there is a considerable delay of cell attachment in VASP(−/−) cells at low fibronectin concentrations.

By flow cytometry quantification we excluded the possibility that this observation was due to different expression levels of the fibronectin-binding β1 and β3 integrins in VASP(−/−) and VASP(+/+) cells (data not shown).

Interestingly, once attached, VASP(−/−) cells adhered to the substrate much tighter than wild-type cells. Thus, VASP(−/−) MCFB needed significantly longer to round up and detach in the presence of trypsin (Fig. 6c) or EDTA (not shown). Taken together, these results strongly suggest that the reorganization of cellular processes required for the transition from a suspended to an adhesive cellular state and vice versa are compromised in the absence of VASP.

FN-coated beads bind stronger to VASP(−/−) fibroblasts

Analysis of the mechanisms that lead to stronger cell adhesion in the absence of VASP is hampered by the fact that these cells are much more spread than their wild-type counterparts, covering about twice the surface area (García Arguinzonis et al. 2002). This leaves two principal possibilities, namely (a) the increased overall contact area is accompanied by a parallel increase in adhesion strength, or (b) cell adhesion is strengthened irrespective of the area of contact with the substrate. To investigate this in more detail, we tested cell adhesion of FN-coated beads, which could be manipulated with laser tweezers. Once settled down, FN-coated beads attached to the cell surfaces within a few seconds, whereas BSA-coated beads did not bind (Fig. 7a). For analysis, beads were grouped into three classes:

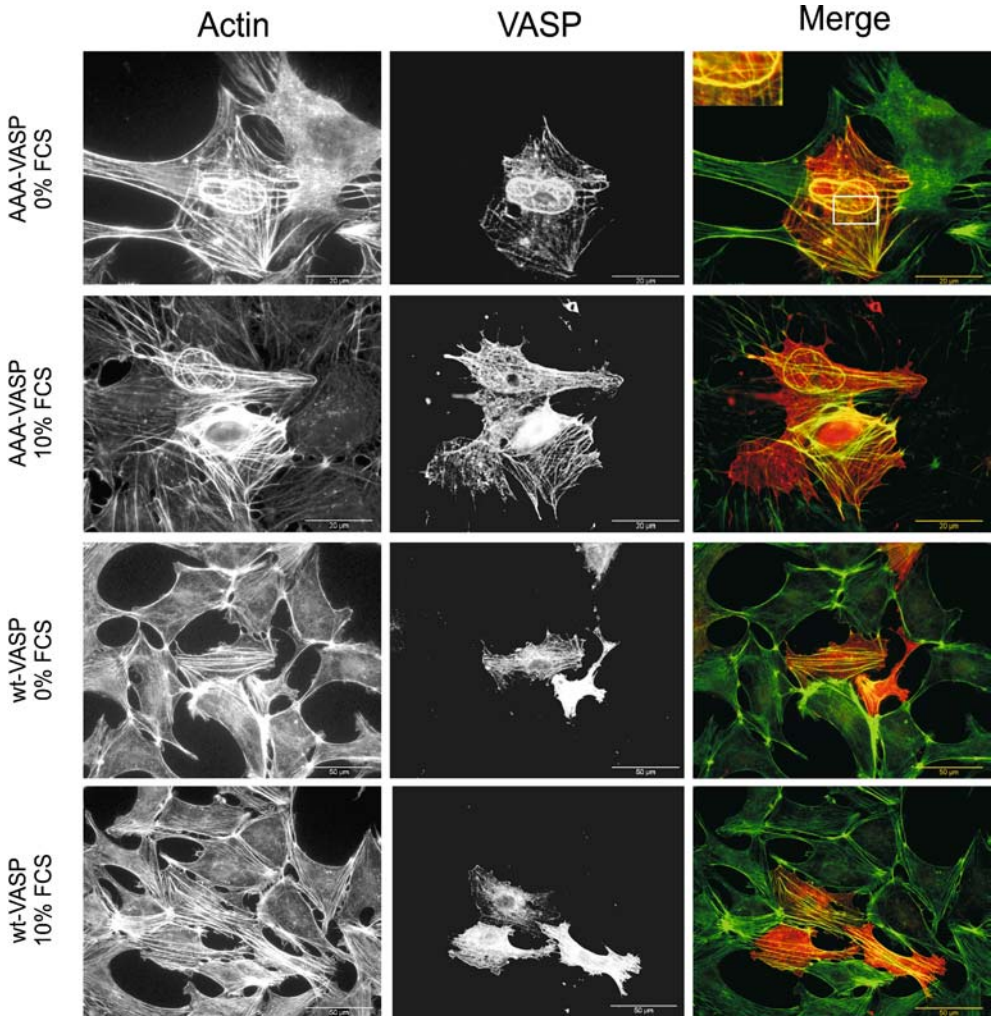

Fig. 5 Stress fibre persistence in VASP-overexpressing cells during serum starvation. PtK_2 cells were transfected with a plasmid encoding either human wild-type VASP or VASP with all three phosphorylation sites for cyclic nucleotide-dependent protein kinases mutated to alanines (AAA-VASP) and cultured for 48 h in the presence or absence of FCS, as indicated. Cells were double-stained with Oregon Green phalloidine for F-actin labelling (*left column*) and an anti-VASP serum to reveal overexpressing cells (*middle column*). A merge of both exposures is shown in the right column. A fraction of the VASP-overexpressing cells shows characteristic F-actin containing filamentous structures in the perinuclear region, one of which has been enlarged in the insert within the upper right frame

I Beads that bound and could not be moved with the laser tweezers set at 40 mW made up the biggest group among both wild-type and VASP-deficient cells.

II "Tethered beads": Irrespective of VASP expression, 19.9% (VASP(+/+) cells) or 19.5% (VASP(−/−) cells) of the beads were elastically bound (40–160 mW laser power) and (at 160 mW laser power) could be moved horizontally over a distance of several μm, elastically returning to a position close to their starting position ("tethered" beads).

III The remaining beads were freely movable and were classified as non-bound.

No major differences were observed between VASP(+/+) and VASP(−/−) fibroblasts, both with the FN ligand and the BSA control (Fig. 7a). FN-coated beads seeded on VASP(−/−) cells appeared to take somewhat longer to attach, which is in agreement with the cell adhesion assay reported above. Firmly attached beads and tethered beads (classes I and II, respectively) together were analysed for whether or not the linkage could be broken with a laser power of 160 mW. Here, VASP(−/−) cells showed a significantly stronger adhesion of FN-coated beads to the cell surface as compared to VASP(+/+) cells ($P < 0.01$ using a binomial test). Once attached to the surfaces of VASP-deficient cells, only 2.8% of the analysed beads (tethered and bound beads) could be torn off, whereas this was possible with 36% of the beads bound to VASP(+/+) cells (Fig. 7b). Again, this is in good agreement with the whole cell adhesion and detachment assay described above.

The interfaces between FN-coated beads and the cell surfaces should be similar sized in wild-type and VASP knockout cells. Therefore, measuring the binding strength of the beads can correct for the increased ECM contact area of the highly spread VASP-deficient cells. Nevertheless, for instance a selective engulfment of the beads by one cell type could account for a significant increase in contact area and binding strength. This possibility has been ruled out by scanning electron microscopy of cell surface bound FN-coated beads. Both, in VASP-deficient and wild type cells, beads were attached to a plane cell surface (Fig. 8, upper panel) where several beads displayed

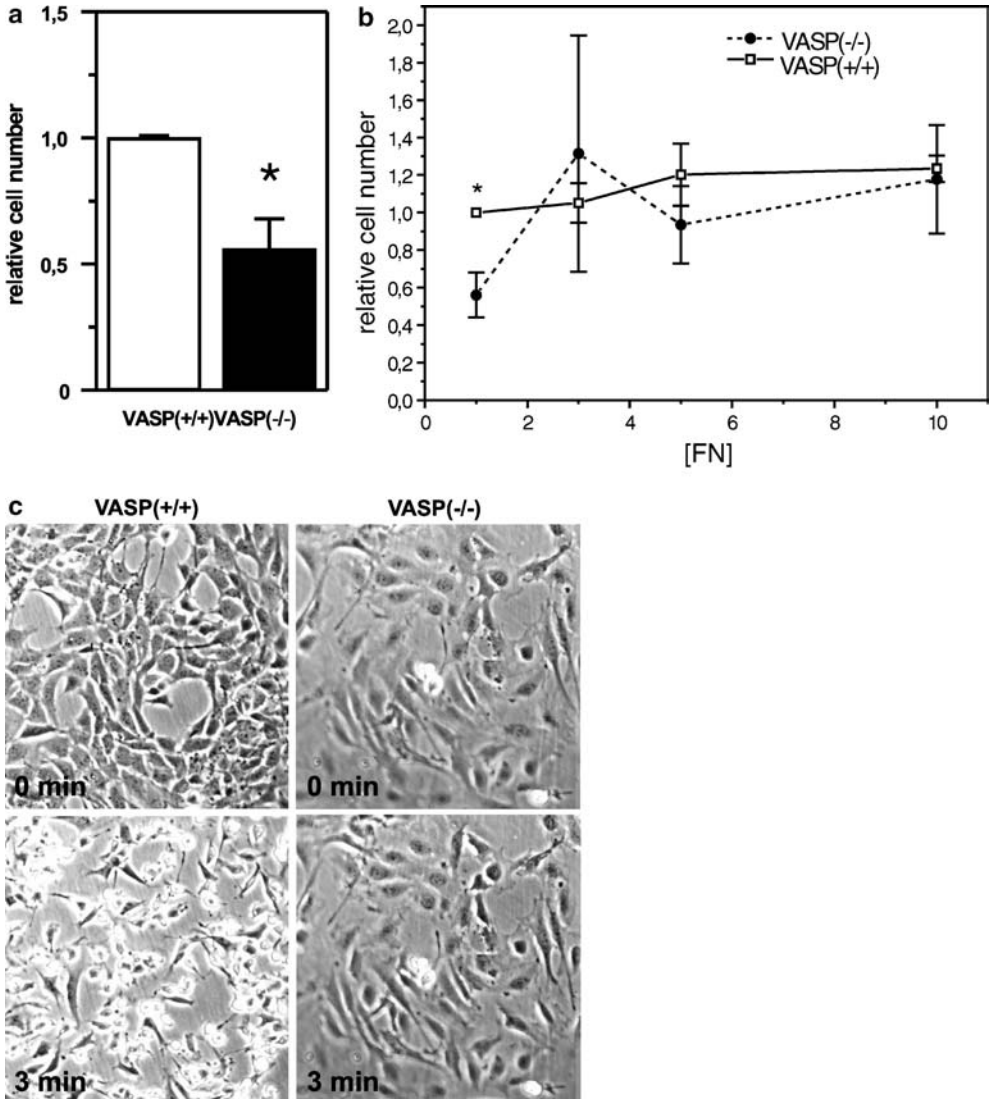

Fig. 6 Decreased cell adhesion and detachment rates in VASP(−/−) MCFB. **a** Relative number of VASP(+/+) cells and VASP(−/−) cells attaching within the first 30 min to microtiter wells coated with 1 μg/ml fibronectin (average of four different experiments ± SEM; $*P < 0.05$). **b** Cell attachment to increasing concentrations of fibronectin. VASP(−/−) (*filled circles*) and VASP(+/+) (*empty squares*) MCFB were seeded into microtiter wells coated with various concentrations [μg/ml] of fibronectin (*FN*). Thirty minutes after seeding, non-adherent cells were washed off and the relative cell numbers of adherent cells were determined (average of fours different experiments ± SEM). ($*P < 0.05$; $**P < 0.005$, unpaired *t* test). **c** Phase contrast micrographs showing that wild-type, but not VASP(−/−) cells, round off and begin to detach within 3 min of incubation in the presence of 0.1% trypsin

contacts with short filopodium-like projections (Fig. 8, lower panel).

Hence, in extension of the whole cell adhesion experiment reported above, utilization of the laser tweezers revealed that cell adhesion per se appears to be strengthened in VASP-deficient cells, irrespective of the increased total cell area in contact with the ECM.

Membrane tethers and membrane rigidity are regulated by VASP

Most likely, the bead-bound surface protuberances that are visible in scanning electron micrographs are the morphological correlates of tethered beads observed in laser tweezers experiments. While the fraction of beads that was bound via elastic tethers was close to 20% in both wild-type and VASP(−/−) cells (Fig. 7a), the resisting force of individual tethers was grossly different. Thus, in wild-type cells most (89.9%) of the tethered beads were movable over several μm with a laser power of 40 mW, whereas in VASP-deficient cells only a minor fraction (14.2%) of the tether-bound beads could be moved with the low-power setting. The elastic binding of the remaining tethers was evident only after increasing the power of the laser tweezers to 160 mW.

Furthermore, the tethers in VASP(+/+) cells were three- to fourfold longer than in VASP-deficient cells at both laser powers (Fig 7c; 40 and 160 mW, respectively). The tether length difference observed was VASP-dependent, since a reconstituted VASP clone with a VASP expression level somewhat lower than wild-type cells (clone G5) (García Arguinzonis et al. 2002) displayed tethers almost as long as VASP(+/+) cells, whereas the phenotype of cells with very low VASP expression (clone E10) was closer to that of VASP(−/−) cells (Fig 7c). Equivalent results were obtained using primary cardiac fibroblasts from both VASP(+/+) and VASP(−/−) animals (not shown), indicating that this is no cell line artefact.

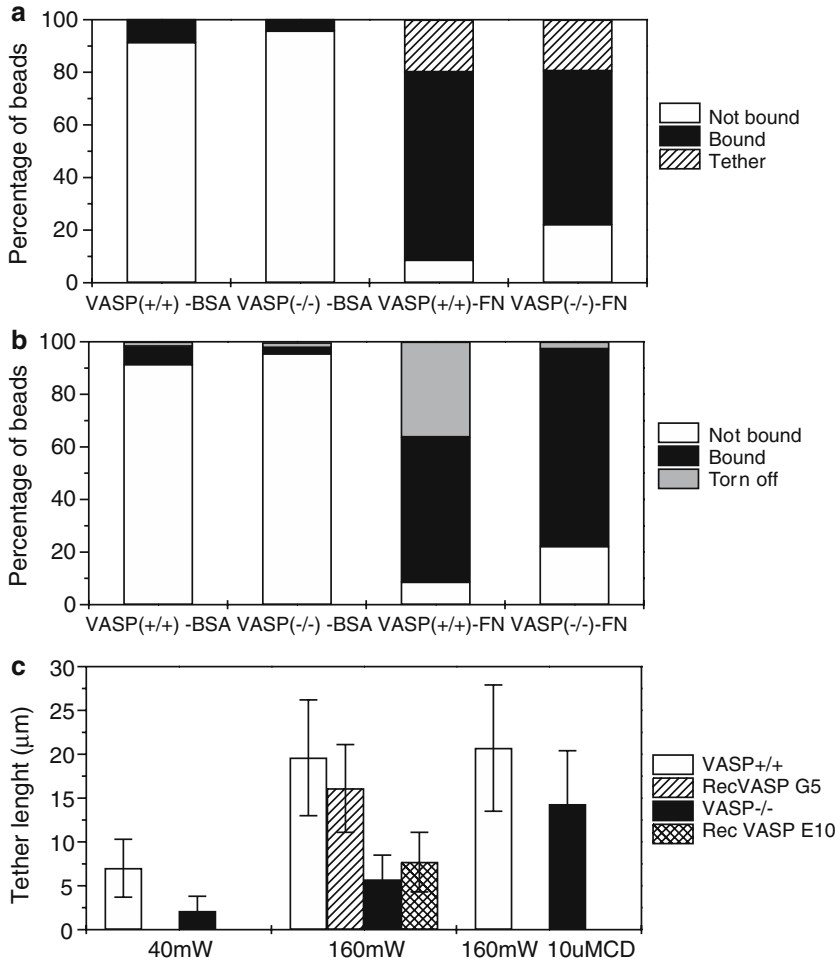

Fig. 7 Increased cell surface adhesiveness of fibronectin-coated beads on VASP(−/−) MCFB. **a** Fibroblasts bind specifically to FN-coated beads. Beads were classified as bound (*black*) when they could not be moved with laser tweezers at 40 mW. A fraction of beads formed membrane tethers when pulling with the laser tweezers (*hatched*). The unbound fraction is shown in white. **b** FN-coated beads adhere stronger to VASP(−/−) cells. Beads did not bind (*white*), or bound weakly (*grey*), i.e. could be torn off, or firmly (*black*), i.e. could not be torn off by pulling with the laser tweezers (160 mW). Three independent experiments were performed and at least a total of 100 beads were counted for each cell type. **c** Tether lengths of fibronectin-coated beads. Tether lengths were measured for VASP(+/+) (*white*), VASP(−/−) (*black*), and VASP(−/−) fibroblasts reconstituted with human VASP (clone G5, physiological level of VASP expression; clone E10, low VASP expression). Experimental conditions were as indicated. 40/160 mW: power setting of laser tweezers, 10 µM CD: pre-incubation with 10 µM cytochalasin D for 30 min. *Error bars* indicate SEM for 11–20 beads, each measured three to five times

Increased membrane tether rigidity in VASP(−/−) cells involves actin cytoskeletal changes

To investigate the contribution of the actin cytoskeleton to the different tether sizes in VASP(−/−) and wild-type cells, we treated the cells with cytochalasin D to disrupt cellular actin filaments. Cells strongly retracted and rounded up after 30 min of pre-incubation with 10 µM cytochalasin D, but remained viable and completely recovered after the removal of the drug (data not shown). After cytochalasin D treatment tether lengths in VASP(+/+) remained unchanged at 20.7 ± 7.2 µM, as compared to 19.6 ± 6.6 µm in control cells. In contrast, the tether lengths of VASP(−/−) fibroblasts increased from 5.7 ± 2.8 to 14.3 ± 6.1 µm upon cytochalasin D treatment (Fig. 7c). This corresponds to about 70% of the average VASP(+/+) tether length. Tether length has been shown previously to increase upon disruption of the actin cytoskeleton by cytochalasins (Raucher and Sheetz 1999). This is consistent with our observations with VASP(−/−), but not VASP(+/+) cells, implying that the actin cytoskeleton is already highly flexible or dynamic in VASP-expressing wild-type cells. These results also demonstrate that actin cytoskeletal changes contribute to a major extent to the increased rigidity of membrane tethers in VASP(−/−) cells.

Probing cell surface mechanical properties by atomic force microscopy

The actin-cytoskeleton largely determines membrane elasticity (reviewed in Sheetz 2001). Therefore, we first examined the cell surface topology of VASP(−/−) and

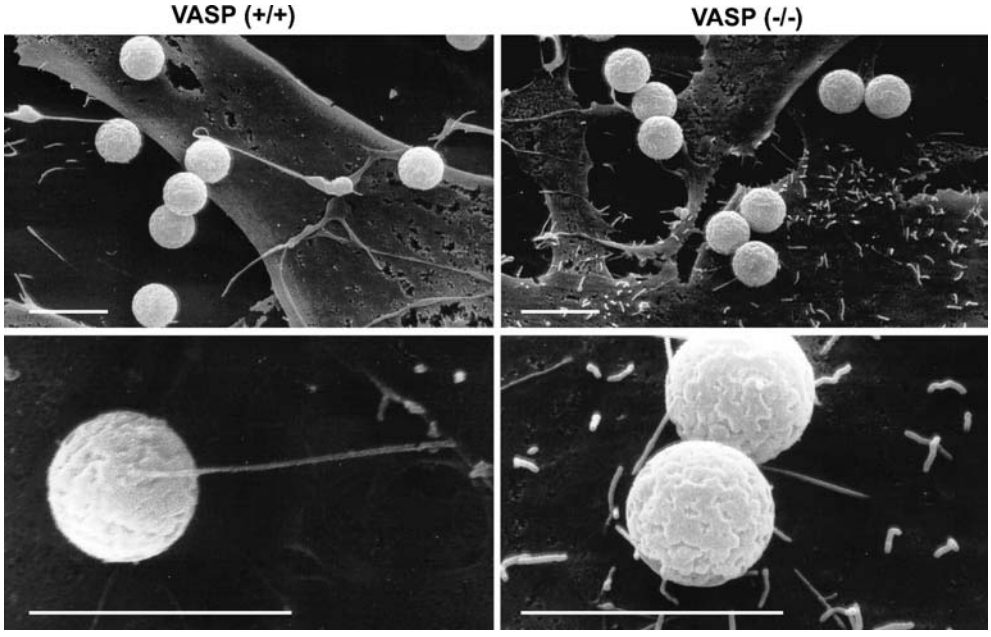

Fig. 8 Scanning electron microscopical analysis of fibronectin-coated beads on wild-type and VASP-deficient cells. Scanning electron micrographs of FN-coated beads attached to VASP(+/+) (*left panel*) or VASP(−/−) fibroblasts (*right panel*). Beads are either directly surface bound (*upper panel*) or linked to the cell surface via membrane projections (*lower panel*), irrespective of the presence or absence of VASP. *Scale bars* 5 μm

VASP(+/+) fibroblasts by atomic force microscopy (AFM, Binnig et al. 1986). Visualization of the primary data reveals large differences in cell morphology between both cell types (Fig. 9a). VASP-deficient cells are much more spread than wild-type cells, whereas the maximal cell heights above the nucleus are similar. Cross-sectional views show that VASP(−/−) cells are much flatter as compared to VASP(+/+) cells (Fig. 9, right panel).

AFM can also be used to measure the elasticity of cells by performing the so-called force-distance cycles (Simon et al. 2003). When the AFM tip comes into contact with the cell surface while moving continuously downwards, the cantilever will be subsequently deflected proportional to the surface stiffness. That means, the steeper a force versus distance plot, the lower the elasticity of the sample. Cell elasticity, as derived from force calibration plots and analysed according to Simon et al. (2003), was found three to four times lower in VASP-deficient cells as compared to VASP(+/+) cells. To exclude the possibility of artefacts due to the close approximation of the AFM tip to the substratum at the extremely thin lamella, particularly in VASP(−/−) cells, measurements were recorded not only at the level of the lamellipodium but also above the nucleus. In both cases similar results were obtained (Fig. 10), which were also reproducible with primary cells (not shown). This indicates that the differences observed are neither an artefact caused by the flatter morphology of VASP-deficient cells nor are they specific for this particular cell line.

The hysteresis between the force versus distance plots occurring during the approach (Fig. 10, ''extending'') and retraction of the cantilever to or from the surface (Fig. 10, ''retracting'') further tells that the elastic forces of VASP(+/+) cells are comparable to viscous forces, while for VASP(−/−) cells, the elastic forces are dominant (''retracting'' and ''extending'' are almost congruent).

Discussion

Cellular remodelling and adhesion

In the present study, we investigated the influence of VASP expression on actin cytoskeletal organization and integrin-dependent cell adhesion. As judged from both laser tweezers and AFM data, the cortical cytoskeleton is more rigid in VASP(−/−) cells. Stress fibre morphology and stability in serum-starved cells strongly suggest that actin cytoskeletal structures in the absence of VASP are also less dynamic.

This is also reflected in cell behaviour:

First, we have reported previously that VASP-deficient cells show a compromised ability to reorient their stress fibres and cell axes and release their rear ends, which results in a poor performance in an in vitro motility assay (García Arguinzonis et al. 2002).

Second, adhesion of VASP-deficient cells to surfaces coated with low concentrations of fibronectin was delayed but quantitative. Delayed adhesion of VASP(−/−) cells suggests that the cellular remodelling required for the transition between adherent and suspended states is impaired in VASP-deficient cells. In line with that notion, stable F-actin formation induced by jasplakinolide leads to a striking increase in neutrophil rigidity, which is associated with a block in fMLP stimulated integrin CD11b surface expression and adhesion on immobilized platelets (Sheikh et al. 1997).

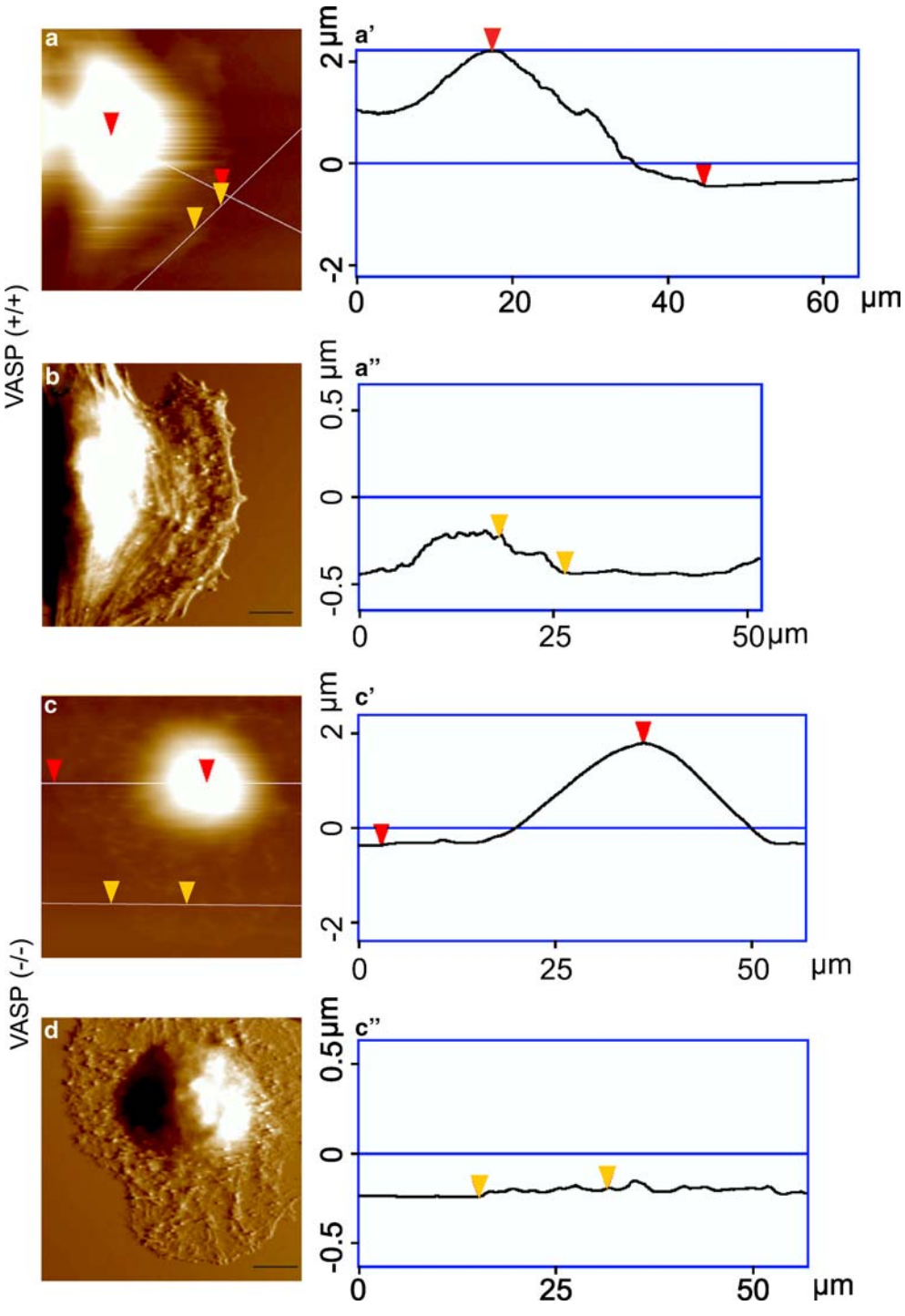

Fig. 9 Surface topology of wild-type cells and VASP(−/−) cells as revealed by atomic force microscopy. *Left panel* Height (**a**, **c**) and deflection (*error*) images (**b**, **d**) of living wild-type and VASP(−/−) fibroblasts. *Right panel* Cross sections through the lamellipodium and through the nucleus as indicated in the *left panel*. Note the much flatter morphology of VASP(−/−) cells as compared to VASP(+/+) fibroblasts. *Scale bars* 15 µm

Strengthening of the actin cytoskeleton in VASP-deficient cells may also affect integrin ligand binding or clustering, which appear to require a transient integrin release from cytoskeletal constraints (Bennett et al. 1999; Calderwood et al. 2000; Nishizaka et al. 2000). Eventually, however, reattachment to the actin cytoskeleton stabilizes integrin-dependent adhesion. Similarly, although the adhesion of VASP-deficient cells was delayed when seeded on low FN concentrations, they finally adhered much stronger than their wild-type counterparts. In VASP-deficient mice integrin-dependent platelet vessel wall interactions are also increased, supporting the in vivo relevance of our findings (Massberg et al. 2004).

To correct the increased contact area of the highly spread VASP-deficient cells (García Arguinzonis et al. 2002), we tested cell surface binding of fibronectin-coated beads. Again, we found a marked increase of binding strength in the absence of VASP. Therefore, adhesion complexes per se appear to be strengthened irrespective of the size of the overall cell contact area. This conclusion

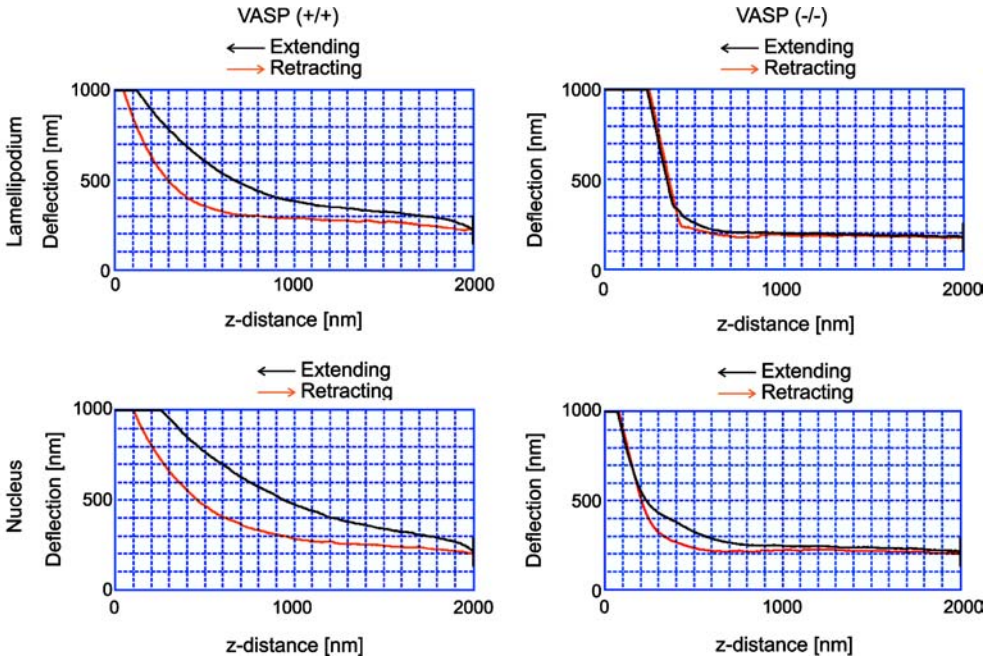

Fig. 10 Probing the surface of VASP(+/+) and VASP(−/−) MCFB by atomic force microscopy. Representative force calibration plots of VASP(+/+) cells (*left panel*) and VASP(−/−) cells (*right panel*) are shown. Measurements were done at the lamellipodium (*upper row*) or nucleus (*lower row*). In both cases note the much stiffer surface of VASP(−/−) cells as compared to VASP(+/+) cells

is also supported by the fact that focal adhesion sites of VASP(−/−) cells are generally bigger than in wild-type cells. As the size of individual focal contacts above a certain threshold is proportional to the local traction force (Balaban et al. 2001), this indicates that the forces acting on cell-matrix adhesion complexes of VASP(−/−) cells are increased accordingly. In parallel, elevated MLC phosphorylation and a dramatic cell surface stiffening of VASP-deficient cells indicate also an increased tensile strength of the actin cytoskeleton. In agreement with our data, there is additional evidence for a rigidification of neurophils that have been loaded with an ActA peptide, which interferes with EVH1 domain-dependent interactions of Ena/VASP proteins (Anderson et al. 2003).

Actually, increased contractility may be the causative event promoting focal adhesion assembly and integrin clustering (Burridge and Chrzanowska-Wodnicka 1996), and in consequence may lead to the strengthening of cell adhesion.

Cell surface rigidity and membrane tethers

With a fraction of the cell bound FN-coated beads elastic membrane tethers of several μm in length could be pulled out of the cell surface. The rigidity of these membrane tethers was dramatically elevated in VASP-deficient cells. Membrane components in the tethers are thought to be separated from their cytoskeletal support (Raucher and Sheetz 1999; Sheetz 2001). On the other hand, transfection of GFP-tagged proteins suggests that certain cellular extensions that can be pulled out by cell surface interactions with a coated needle may contain both actin- and microtubule-based elements and might contract by an acto-myosin-type mechanism (Heidemann et al. 1999).

Overall, forces acting on the tethered beads are increasing with the distances the beads are pulled away from the cell surface, with a strong increase towards the end (Raucher and Sheetz 1999). In between, however, over a certain range of tether lengths the restraining forces do not depend on the tether length. Based on the latter observation the presence of a membrane reservoir has been postulated, with the tether length being a direct measure for the size of this reservoir (Raucher and Sheetz 1999). In our system tethers could be extended by a factor of 2–3, both in the presence or absence of VASP, when the power setting of the laser tweezers was increased from 40 to 160 mW. This indicates that the extension of the tethers at least over the last two-thirds to three-quarter of their lengths had to overcome a higher resisting force. Therefore, the postulated membrane reservoir appears to be depleted at an earlier time point. The apparent reservoir size has been suggested to be affected by the intensity of membrane–cytoskeleton interactions and/or cytoskeletal rigidity (Raucher and Sheetz 1999; Sheetz 2001). It is directly evident how cytoskeletal interactions with the plasma membrane may contribute to the resisting force of membrane tethers. Also increased rigidity or contractility of the cell cortex may have similar consequences. Thus, the stiffening of cell shape and cell surface topology has been envisaged to resist the incorporation of plasma membrane into tethers, which otherwise could become available upon cell rounding or from the dissolution of cell surface invaginations, surface folds, or membrane ruffles, or after incorporation of internal membrane stores (Burwen and Satir 1977; Escolar et al. 1989; Raucher and Sheetz 1999). As a corollary, the amount of membrane that could be pulled into membrane tethers of the rigid VASP-deficient cells was markedly

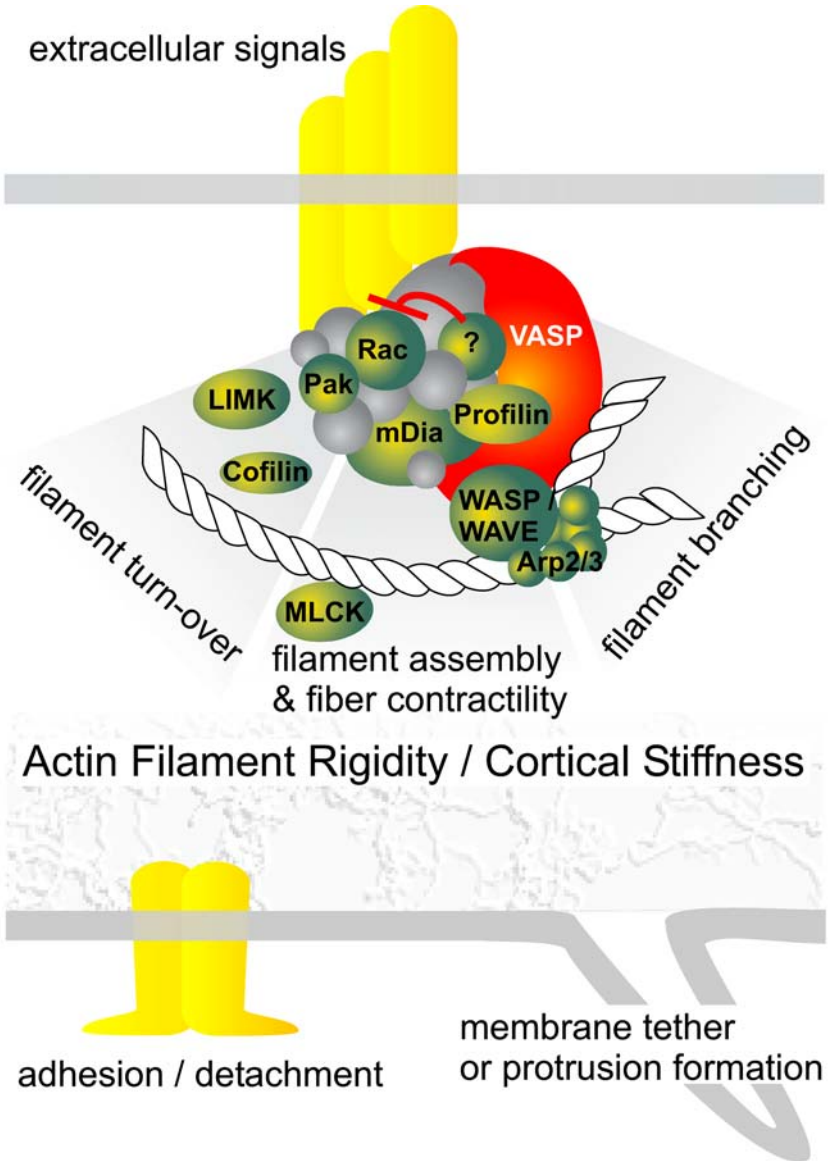

Fig. 11 A model, suggesting VASP as a scaffold protein. Besides its direct interactions with actin and actin regulating proteins, VASP enables the formation of signalling complexes that modulate actin cytoskeletal rigidity and cortical stiffness. The mechanical properties of the actin cytoskeleton, in turn, affect integrin-dependent adhesion as well as the formation of membrane tethers and cell surface protrusions

lower than with the smoother wild-type cells, and was directly correlated with the amount of VASP expression in two different reconstituted cell clones.

Interestingly, increased membrane tension has been suggested to down-regulate lamellipodial extension rates (Raucher and Sheetz 2000; Sheetz 2001), consistent with the decreased lamellipodia protrusion velocity in Ena/VASP-deficient cells (Bear et al. 2002), which therefore might be secondary to the alteration of cytoskeletal tension. We hypothesize that Ena/VASP-dependent modulation of membrane tension may be a major factor regulating the formation and retraction of lamellipodia, filopodia, neurites, and other membrane processes in response to extracellular cues (Fig. 11). This is particularly appealing in view of Ena/VASP protein functions in axon guidance (Bashaw et al. 2000; Colavita and Culotti 1998) and the role of substrate–cytoskeletal coupling in the regulation of growth cone motility and guiding (Suter and Forscher 2000).

Direct versus indirect VASP action

Considering possible mechanisms that could mediate alterations of the actin cytoskeleton in VASP-deficient and VASP-overexpressing cells, respectively, there are two principle possibilities. First, VASP is a known actin binding and bundling protein (Bachmann et al. 1999; Harbeck et al. 2000; Reinhard et al. 1992; Walders-Harbeck et al. 2002) and may exert a direct effect on actin filament formation, dynamics, and supramolecular organization. Second, VASP modulates signal transduction pathways that affect the actin cytoskeleton (García Arguinzonis et al. 2002). In particular, with respect to the first possibility, Ena/VASP proteins have been suggested to stabilize actin filaments against severing by Gelsolin (Bearer et al. 2000) to oppose the action of capping protein (Bear et al. 2002), and to facilitate the release of branched actin filaments from a filament-branching enzyme (Samarin et al. 2003). The

latter mechanisms would thus enable continuous filament elongation, whereas in the absence of Ena/VASP proteins filaments are shorter with a higher degree of branching (Bear et al. 2002; Skoble et al. 2001). Ostensibly, this could account for the increase in cortical actin network stiffness. However, this effect is likely to be more distinctive at a highly branched, very narrow zone directly proximal to the leading edge as compared to the remainder of the lamellipodium and cell surface, where cofilin/ADF-mediated debranching is thought to prevail (Pollard and Borisy 2003). In addition, the more stable and hence more persistent plasma membrane protrusions observed in Ena/VASP-deficient cells (Bear et al. 2002) could indirectly lead to a stronger integrin–cytoskeleton coupling and improvement of cell adhesion as observed in the present study (Choquet et al. 1997; Griffiths and Penninger 2002; Krause et al. 2002; Nishizaka et al. 2000).

However, our data clearly demonstrate that such a mechanism alone cannot account for all aspects of increased cytoskeletal rigidity and stability that we observed: Increased MLC phosphorylation (Fig. 3) and elevated Rac and PAK activity (García Arguinzonis et al. 2002) in VASP(−/−) cells favour the second possibility, namely an indirect action through regulation of signalling pathways to the actin cytoskeleton. Indeed, another finding also suggests an indirect effect. Thus, wild-type VASP and AAA-VASP (this study), and even VASP constructs that lack a C-terminal part essential for multimerization and actin bundling in vitro (Bachmann et al. 1999) lead to thicker stress fibres when overexpressed (Grosse et al. 2003; Price and Brindle 2000). VASP overexpression also stabilizes stress fibres (Figs. 2e–f, 5).

VASP has properties of a scaffold protein

Thicker and more stable stress fibres observed in VASP-overexpressing cells closely resemble the stress fibre phenotype of VASP(−/−) cells (Fig. 2a–c). Actually, phenomena of this kind, i.e. both elevated and decreased expression levels having similar cellular effects, are regarded as a major criterion for the involvement of scaffold proteins (Burack and Shaw 2000; Levchenko et al. 2000). This is based on the fact that any deviation (i.e. increase or decrease) from a balanced stoichiometric ratio of a scaffold to its binding partners will be less effective in forming a functional signalling complex. Therefore, VASP has properties of a scaffold protein and could enable the close encounter and mutual regulation of its binding partners, among them numerous signalling proteins (Reinhard et al. 2001). For instance, there is sustained activation of Rac and its downstream target PAK in VASP(−/−) cells (García Arguinzonis et al. 2002) and overexpression of VASP results in the activation of membrane ruffling (Price and Brindle 2000) suggesting Rac activation in these cells as well. This is also reminiscent of the situation with *Dictyostelium* mutants that are either deficient for the VASP family member DdVASP or overexpress the protein and produce more lateral pseudopodia in both cases (Han et al. 2002). Expression of constitutively active PAK in microvascular endothelial cells leads to an increase in stress fibres, focal adhesions, and MLC phosphorylation (Kiosses et al. 1999), similar to our observation with VASP-deficient MCFB. In addition, microvascular endothelial cells expressing constitutively active PAK show increased contractility (Kiosses et al. 1999). This resembles the situation found with both VASP-deficient and VASP-overexpressing cells, where cortical actin cytoskeleton tension of VASP(−/−) cells and the stress fibre phenotype of both cell types also argues for increased cell contractility. As a downstream target of PAK, LIM kinase inactivates the actin filament severing proteins Cofilin/ADF by phosphorylation and thus stabilizes actin filaments (Bamburg 1999). Most intriguingly, cofilin also has debranching activity (Blanchoin et al. 2000; Pollard and Borisy 2003). It is therefore conceivable that in VASP(−/−) cells elevated Rac/PAK pathway activity results in cofilin/ADF inactivation, which could contribute to both, enhanced filament branching (Bear et al. 2002) and stress fibre stabilization (this study), and as a consequence also to increased lamellipodial persistence (Bear et al. 2002).

In conclusion, our results reveal that VASP affects stress fibre stability and cortical actin cytoskeleton rigidity, as well as cell adhesion and detachment, with the modulation of actin cytoskeletal turnover and contractility as possible common mechanisms. Moreover, we presented several lines of evidence revealing that, beyond a direct interaction with cytoskeletal structures, VASP also modulates signalling to the actin cytoskeleton.

Acknowledgments The authors thank Elke Baumeister, Agnes Weth, Elke Butt, and Stepan Gambaryan for help and reagents, and Ulrich Walter for continuous support and discussions. This work was supported by the Deutsche Forschungsgemeinschaft (SFB 487 B4 & B5, SFB 355 B4 & C8, and Re1011/3-2).

References

Abassi YA, Vuori K (2002) Tyrosine 221 in Crk regulates adhesion-dependent membrane localization of Crk and Rac and activation of Rac signaling. Embo J 21:4571–4582

Anderson SI, Behrendt B, Machesky LM, Insall RH, Nash GB (2003) Linked regulation of motility and integrin function in activated migrating neutrophils revealed by interference in remodelling of the cytoskeleton. Cell Motil Cytoskeleton 54:135–146

Arthur WT, Noren NK, Burridge K (2002) Regulation of Rho family GTPases by cell-cell and cell-matrix adhesion. Biol Res 35:239–246

Aszodi A, Pfeifer A, Ahmad M, Glauner M, Zhou XH, Ny L, Andersson KE, Kehrel B, Offermanns S, Fassler R (1999) The vasodilator-stimulated phosphoprotein (VASP) is involved in cGMP- and cAMP-mediated inhibition of agonist-induced platelet aggregation, but is dispensable for smooth muscle function. Embo J 18:37–48

Auerbuch V, Loureiro JJ, Gertler FB, Theriot JA, Portnoy DA (2003) Ena/VASP proteins contribute to Listeria monocytogenes pathogenesis by controlling temporal and spatial persistence of bacterial actins-based motility. Mol Microbiol 49:1361–1375

Bachmann C, Fischer L, Walter U, Reinhard M (1999) The EVH2 domain of the vasodilator-stimulated phosphoprotein mediates tetramerization, F-actin binding, and actin bundle formation. J Biol Chem 274:23549–23557

Balaban NQ, Schwarz US, Riveline D, Goichberg P, Tzur G, Sabanay I, Mahalu D, Safran S, Bershadsky A, Addadi L, Geiger B (2001) Force and focal adhesion assembly: a close relationship studied using elastic micropatterned substrates. Nat Cell Biol 3:466–472

Bamburg JR (1999) Proteins of the ADF/cofilin family: essential regulators of actin dynamics. Annu Rev Cell Dev Biol 15:185–230

Bashaw GJ, Kidd T, Murray D, Pawson T, Goodman CS (2000) Repulsive axon guidance: abelson and enabled play opposing roles downstream of the roundabout receptor. Cell 101:703–715

Baumgartner W, Schutz GJ, Wiegand J, Golenhofen N, Drenckhahn D (2003) Cadherin function probed by laser tweezer and single molecule fluorescence in vascular endothelial cells. J Cell Sci 116:1001–1011

Bear JE, Loureiro JJ, Libova I, Fassler R, Wehland J, Gertler FB (2000) Negative regulation of fibroblast motility by Ena/VASP proteins. Cell 101:717–728

Bear JE, Svitkina TM, Krause M, Schafer DA, Loureiro JJ, Strasser GA, Maly IV, Chaga OY, Cooper JA, Borisy GG, Gertler FB (2002) Antagonism between Ena/VASP proteins and actin filament capping regulates fibroblast motility. Cell 109:509–521

Bearer EL, Prakash JM, Manchester RD, Allen PG (2000) VASP protects actin filaments from gelsolin: an in vitro study with implications for platelet actin reorganizations. Cell Motil Cytoskeleton 47:351–364

Bennett JS, Zigmond S, Vilaire G, Cunningham ME, Bednar B (1999) The platelet cytoskeleton regulates the affinity of the integrin alpha(IIb)beta(3) for fibrinogen. J Biol Chem 274:25301–25307

Binnig G, Quate CF, Gerber C (1986) Atomic force microscope. Physical Review Letters 56:930–933

Bishop AL, Hall A (2000) Rho GTPases and their effector proteins. Biochem J 348 (Pt 2):241–255

Blanchoin L, Pollard TD, Mullins RD (2000) Interactions of ADF/cofilin, Arp2/3 complex, capping protein and profilin in remodeling of branched actin filament networks. Curr Biol 10:1273–1282

Burack WR, Shaw AS (2000) Signal transduction: hanging on a scaffold. Curr Opin Cell Biol 12:211–216

Burridge K, Chrzanowska-Wodnicka M (1996) Focal adhesions, contractility, and signaling. Annu Rev Cell Dev Biol 12:463–518

Burwen SJ, Satir BH (1977) Plasma membrane folds on the mast cell surface and their relationship to secretory activity. J Cell Biol 74:690–697

Calderwood DA, Shattil SJ, Ginsberg MH (2000) Integrins and actin filaments: reciprocal regulation of cell adhesion and signaling. J Biol Chem 275:22607–22610

Castellano F, Le Clainche C, Patin D, Carlier MF, Chavrier P (2001) A WASp-VASP complex regulates actin polymerization at the plasma membrane. Embo J 20:5603–5614

Chew TL, Masaracchia RA, Goeckeler ZM, Wysolmerski RB (1998) Phosphorylation of non-muscle myosin II regulatory light chain by p21- activated kinase (gamma-PAK). J Muscle Res Cell Motil 19:839–854

Choquet D, Felsenfeld DP, Sheetz MP (1997) Extracellular matrix rigidity causes strengthening of integrin–cytoskeleton linkages. Cell 88:39–48

Colavita A, Culotti JG (1998) Suppressors of ectopic UNC-5 growth cone steering identify eight genes involved in axon guidance in *Caenorhabditis elegans*. Dev Biol 194:72–85

del Pozo MA, Price LS, Alderson NB, Ren XD, Schwartz MA (2000) Adhesion to the extracellular matrix regulates the coupling of the small GTPase Rac to its effector PAK. Embo J 19:2008–2014

del Pozo MA, Kiosses WB, Alderson NB, Meller N, Hahn KM, Schwartz MA (2002) Integrins regulate GTP-Rac localized effector interactions through dissociation of Rho-GDI. Nat Cell Biol 4:232–239

del Pozo MA, Alderson NB, Kiosses WB, Chiang HH, Anderson RG, Schwartz MA (2004) Integrins regulate Rac targeting by internalization of membrane domains. Science 303:839–842

Escolar G, Leistikow E, White JG (1989) The fate of the open canalicular system in surface and suspension-activated platelets. Blood 74:1983–1988

Fukata M, Nakagawa M, Itoh N, Kawajiri A, Yamaga M, Kuroda S, Kaibuchi K (2001) Involvement of IQGAP1, an effector of Rac1 and Cdc42 GTPases, in cell–cell dissociation during cell scattering. Mol Cell Biol 21:2165–2183

Gambaryan S, Hauser W, Kobsar A, Glazova M, Walter U (2001) Distribution, cellular localization, and postnatal development of VASP and Mena expression in mouse tissues. Histochem Cell Biol 116:535–543

García Arguinzonis MI, Galler AB, Walter U, Reinhard M, Simm A (2002) Increased spreading, Rac/p21-activated kinase (PAK) activity, and compromised cell motility in cells deficient in vasodilator-stimulated phosphoprotein (VASP). J Biol Chem 277:45604–45610

Geiger B, Bershadsky A (2001) Assembly and mechanosensory function of focal contacts. Curr Opin Cell Biol 13:584–592

Geiger B, Bershadsky A, Pankov R, Yamada KM (2001) Transmembrane crosstalk between the extracellular matrix–cytoskeleton crosstalk. Nat Rev Mol Cell Biol 2:793–805

Geiger B, Bershadsky A (2002) Exploring the neighborhood: adhesion-coupled cell mechanosensors. Cell 110:139–142

Gitai Z, Yu TW, Lundquist EA, Tessier-Lavigne M, Bargmann CI (2003) The netrin receptor UNC-40/DCC stimulates axon attraction and outgrowth through enabled and, in parallel, Rac and UNC-115/AbLIM. Neuron 37:53–65

Griffiths EK, Penninger JM (2002) Communication between the TCR and integrins: role of the molecular adapter ADAP/Fyb/Slap. Curr Opin Immunol 14:317–322

Grosse R, Copeland JW, Newsome TP, Way M, Treisman R (2003) A role for VASP in RhoA-Diaphanous signalling to actin dynamics and SRF activity. Embo J 22:3050–3061

Han YH, Chung CY, Wessels D, Stephens S, Titus MA, Soll DR, Firtel RA (2002) Requirement of a vasodilator-stimulated phosphoprotein family member for cell adhesion, the formation of filopodia, and chemotaxis in dictyostelium. J Biol Chem 277:49877–49887

Harbeck B, Huttelmaier S, Schluter K, Jockusch BM, Illenberger S (2000) Phosphorylation of the vasodilator-stimulated phosphoprotein (VASP) regulates its interaction with actin. J Biol Chem 275:30817–30825

Hauser W, Knobeloch KP, Eigenthaler M, Gambaryan S, Krenn V, Geiger J, Glazova M, Rohde E, Horak I, Walter U, Zimmer M (1999) Megakaryocyte hyperplasia and enhanced agonist-induced platelet activation in vasodilator-stimulated phosphoprotein knockout mice. Proc Natl Acad Sci USA 96:8120–8125

Heidemann SR, Kaech S, Buxbaum RE, Matus A (1999) Direct observations of the mechanical behaviors of the cytoskeleton in living fibroblasts. J Cell Biol 145:109–122

Hüttelmaier S, Harbeck B, Steffens O, Messerschmidt T, Illenberger S, Jockusch BM (1999) Characterization of the actin binding properties of the vasodilator-stimulated phosphoprotein VASP. FEBS Lett 451:68–74

Juliano RL (2002) Signal transduction by cell adhesion receptors and the cytoskeleton: functions of integrins, cadherins, selectins, and immunoglobulin-superfamily members. Annu Rev Pharmacol Toxicol 42:283–323

Kiosses WB, Daniels RH, Otey C, Bokoch GM, Schwartz MA (1999) A role for p21-activated kinase in endothelial cell migration. J Cell Biol 147:831–844

Krause M, Bear JE, Loureiro JJ, Gertler FB (2002) The Ena/VASP enigma. J Cell Sci 115:4721–4726

Krugmann S, Jordens I, Gevaert K, Driessens M, Vandekerckhove J, Hall A (2001) Cdc42 induces filopodia by promoting the formation of an IRSp53:Mena complex. Curr Biol 11:1645–1655

Legg JA, Machesky LM (2004) MRL proteins: leading Ena/VASP to Ras GTPases. Nat Cell Biol 6:1015–1017

Levchenko A, Bruck J, Sternberg PW (2000) Scaffold proteins may biphasically affect the levels of mitogen-activated protein kinase signaling and reduce its threshold properties. Proc Natl Acad Sci USA 97:5818–5823

Liddington RC, Bankston LA, de Pereda JM (2003) Cell adhesion: a FERM grasp of membrane dynamics. Curr Biol 13:R94–R95

Massberg S, Gruener S, Konrad I, García Arguinzonis MI, Eigenthaler M, Hemler K, Kersting J, Schulz C, Mueller I, Besta F, Nieswandt B, Heinzmann U, Walter U, Gawaz M (2004) Enhanced in vivo platelet adhesion in vasodilator-stimulated phosphoprotein (VASP)-deficient mice. Blood 103:136–142

Nishizaka T, Shi Q, Sheetz MP (2000) Position-dependent linkages of fibronectin-integrin-cytoskeleton. Proc Natl Acad Sci USA 97:692–697

Nobes CD, Hall A (1995) Rho, rac, and cdc42 GTPases regulate the assembly of multimolecular focal complexes associated with actin stress fibers, lamellipodia, and filopodia. Cell 81:53–62

Pollard TD, Borisy GG (2003) Cellular motility driven by assembly and disassembly of actin filaments. Cell 112:453–465

Price CJ, Brindle NP (2000) Vasodilator-stimulated phosphoprotein is involved in stress-fiber and membrane ruffle formation in endothelial cells. Arterioscler Thromb Vasc Biol 20:2051–2016

Price LS, Leng J, Schwartz MA, Bokoch GM (1998) Activation of Rac and Cdc42 by integrins mediates cell spreading. Mol Biol Cell 9:1863–1871

Raucher D, Sheetz MP (1999) Characteristics of a membrane reservoir buffering membrane tension. Biophys J 77:1992–2002

Raucher D, Sheetz MP (2000) Cell spreading and lamellipodial extension rate is regulated by membrane tension. J Cell Biol 148:127–136

Raucher D, Stauffer T, Chen W, Shen K, Guo S, York JD, Sheetz MP, Meyer T (2000) Phosphatidylinositol 4,5-bisphosphate functions as a second messenger that regulates cytoskeleton-plasma membrane adhesion. Cell 100:221–228

Reinhard M, Halbrügge M, Scheer U, Wiegand C, Jockusch BM, Walter U (1992) The 46/50 kDa phosphoprotein VASP purified from human platelets is a novel protein associated with actin filaments and focal contacts. Embo J 11:2063–2070

Reinhard M, Jarchau T, Walter U (2001) Actin-based motility: stop and go with Ena/VASP proteins. Trends Biochem Sci 26:243–249

Ridley AJ (2001) Rho GTPases and cell migration. J Cell Sci 114:2713–2722

Samarin S, Romero S, Kocks C, Didry D, Pantaloni D, Carlier MF (2003) How VASP enhances actin-based motility. J Cell Biol 163:131–142

Sheetz MP (2001) Cell control by membrane–cytoskeleton adhesion. Nat Rev Mol Cell Biol 2:392–396

Sheikh S, Gratzer WB, Pinder JC, Nash GB (1997) Actin polymerisation regulates integrin-mediated adhesion as well as rigidity of neutrophils. Biochem Biophys Res Commun 238:910–915

Simon A, Cohen-Bouhacina T, Porte MC, Aime JP, Amedee J, Bareille R, Baquey C (2003) Characterization of dynamic cellular adhesion of osteoblasts using atomic force microscopy. Cytometry 54A:36–47

Skoble J, Auerbuch V, Goley ED, Welch MD, Portnoy DA (2001) Pivotal role of VASP in Arp2/3 complex-mediated actin nucleation, actin branch-formation, and *Listeria monocytogenes* motility. J Cell Biol 155:89–100

Smolenski A, Poller W, Walter U, Lohmann SM (2000) Regulation of human endothelial cell focal adhesion sites and migration by cGMP-dependent protein kinase I. J Biol Chem 275:25723–25732

Suter DM, Forscher P (2000) Substrate–cytoskeletal coupling as a mechanism for the regulation of growth cone motility and guidance. J Neurobiol 44:97–113

von Wichert G, Haimovich B, Feng GS, Sheetz MP (2003) Force-dependent integrin-cytoskeleton linkage formation requires downregulation of focal complex dynamics by Shp2. Embo J 22:5023–5035

Walders-Harbeck B, Khaitlina SY, Hinssen H, Jockusch BM, Illenberger S (2002) The vasodilator-stimulated phosphoprotein promotes actin polymerisation through direct binding to monomeric actin. FEBS Lett 529:275–280

Wessel D, Flugge UI (1984) A method for the quantitative recovery of protein in dilute solution in the presence of detergents and lipids. Anal Biochem 138:141–143

Yu TW, Hao JC, Lim W, Tessier-Lavigne M, Bargmann CI (2002) Shared receptors in axon guidance: SAX-3/Robo signals via UNC-34/Enabled and a netrin-independent UNC-40/DCC function. Nat Neurosci 5:1147–1154